Available online at www.sciencedirect.com
ScienceDirect
Methods 44 (2008) 205–221
METHODS
www.elsevier.com/locate/ymeth

Apoptosis and necrosis: Detection, discrimination and phagocytosis

Dmitri V. Krysko [a,b], Tom Vanden Berghe [a,b], Katharina D'Herde [c], Peter Vandenabeele [a,b,*]

[a] Molecular Signaling and Cell Death Unit, Department for Molecular Biomedical Research, VIB, 9052 Ghent, Belgium
[b] Department of Molecular Biology, Ghent University, 9052 Ghent, Belgium
[c] Department of Anatomy, Embryology, Histology and Medical Physics, Ghent University, 9000 Ghent, Belgium

Accepted 21 December 2007

Abstract

Three major morphologies of cell death have been described: apoptosis (type I), cell death associated with autophagy (type II) and necrosis (type III). Apoptosis and cell death associated with autophagy can be distinguished by certain biochemical events. However, necrosis is characterized mostly in negative terms by the absence of caspase activation, cytochrome *c* release and DNA oligonucleosomal fragmentation. A particular difficulty in defining necrosis is that in the absence of phagocytosis apoptotic cells become secondary necrotic cells with many morphological features of primary necrosis. In this review, we present a selection of techniques that can be used to identify necrosis and to discriminate it from apoptosis. These techniques rely on the following cell death parameters: (1) morphology (time-lapse and transmission electron microscopy and flow fluorocytometry); (2) cell surface markers (phosphatidylserine exposure versus membrane permeability by flow fluorocytometry); (3) intracellular markers (oligonucleosomal DNA fragmentation by flow fluorocytometry, caspase activation, Bid cleavage and cytochrome *c* release by western blotting); (4) release of extracellular markers in the supernatant (caspases, HMGB-1 and cytokeratin 18). Finally, we report on methods that can be used to examine interactions between dying cells and phagocytes. We illustrate a quantitative method for detecting phagocytosis of dying cells by flow fluorocytometry. We also describe a recently developed approach based on the use of fluid phase tracers and different kind of microscopy, transmission electron and fluorescence microscopy, to characterize the mechanisms used by phagocytes to internalize dying cells.

Keywords: Apoptosis; Necrosis; Autophagy; Cell death; Phagocytosis; Macropinocytosis; Caspases; DNA fragmentation; Cytokeratin 18; HMGB-1; Phosphatidylserine; Methods

1. Introduction

Homeostasis is maintained in multicellular organisms by a balance between cell proliferation and cell death. Several types of cell death have been described: apoptosis (type I), cell death associated with autophagy (type II), necrosis or oncosis (type III), mitotic catastrophe, anoikis, excitotoxicity, Wallerian degeneration, and cornification of the skin [1]. The final fate of almost any dying/dead cells regardless of death type is engulfment by non-professional or professional phagocytes [2]. This clearance process is of outmost importance for the development and homeostasis of organisms because defective or inefficient clearance may contribute to several human pathologies, including systemic lupus erythematosus [3], cystic fibrosis [4] and chronic obstructive pulmonary disease [5].

Cells undergoing apoptosis show typical, well-defined morphological changes, including plasma membrane blebbing, chromatin condensation with margination of chromatin to the nuclear membrane, karyorhexis (nuclear fragmentation), and formation of apoptotic bodies [6]. Apoptosis has been characterized by several biochemical criteria, including different kinetics of phosphatidylserine (PS) exposure on the outer leaflet of the plasma membrane [7,8], changes in mitochondrial membrane permeability [9],

* Corresponding author. Address: Department for Molecular Biomedical Research, VIB-Ghent University, Technologiepark 927, B-9052 Ghent (Zwijnaarde), Belgium. Fax: +32 9 3313609.
E-mail address: Peter.Vandenabeele@dmbr.UGent.be (P. Vandenabeele).

1046-2023/$ - see front matter © 2008 Elsevier Inc. All rights reserved.
doi:10.1016/j.ymeth.2007.12.001

release of intermembrane space mitochondrial proteins [10], and caspase-dependent activation and nuclear translocation of a caspase-activated DNase resulting in internucleosomal DNA cleavage [11]. Identification of these morphological and biochemical markers of apoptosis makes it possible to distinguish it from other forms of cell death.

Cells undergoing death associated with autophagy are characterized by the presence of double membrane autophagic vacuoles. Autophagy is foremost a survival mechanism that is activated in cells subjected to nutrient or obligate growth factor deprivation. When cellular stress continues, cell death may continue by autophagy alone, or else it often becomes associated with features of apoptotic or necrotic cell death [12]. Specific biochemical markers have been determined for cell death associated with autophagy, such as delocalization of GFP-LC3 to the autophagosomes [13] or the lipidation of LC3, as detected by band shift in western blots [14,15].

In contrast, necrosis is characterized by rapid cytoplasmic swelling and is therefore also often referred to as oncosis. It culminates in rupture of the plasma membrane and organelle breakdown [16]. Necrosis has long been described as a consequence of extreme physicochemical stress, such as heat, osmotic shock, mechanical stress, freeze thawing and high concentration of hydrogen peroxide. In these conditions, cell death occurs quickly due to the direct effect of the stress on the cell, and therefore this cell death process has been described as accidental and uncontrolled. However, many different cellular stimuli (TNF on certain cell lines, dsRNA, IFN-γ, ATP depletion, ischemia) have been shown to induce a necrotic process that follows defined steps and signaling events reminiscent of a true cell death program [17]. This induced necrotic cell death results from extensive cross-talk between several biochemical and molecular events at different cellular levels, and it is as controlled and programmed as apoptosis (reviewed in [18]). It is important to distinguish necrosis from other forms of cell death, particularly because it is often associated with unwarranted loss of cells in human pathologies [18–20]. It can also lead to local inflammation due to release from dead cells of intracellular factors, the so-called damage associated molecular patterns that alert the innate immune system. However, there is no clear biochemical definition of necrotic cell death and consequently no positive biochemical makers that unambiguously discriminate necrosis from apoptosis. Another problem is that even the interpretation of dying cell morphology may be complex, because in the absence of phagocytosis apoptotic cells proceed to a stage called secondary necrosis, which shares many features of primary necrosis. In this review we describe a selection of techniques for discrimination of necrosis from apoptosis, and we stress that accurate discrimination is only possible through an integrated approach based on several morphological and biochemical parameters.

2. Methods for analysis of cell morphology

In this section we will describe the use of time-lapse microscopy, flow fluorocytometry and transmission electron microscopy as means for distinguishing between apoptotic and necrotic cell death by analyzing cell morphology. Throughout this article we will use as an example the L929sA fibrosarcoma cell line, in which apoptotic as well as necrotic cell death can be induced. Necrotic cell death is induced in L929sA cells by stimulation of TNFR1, whereas in L929sA cells transfected with human Fas (L929sAhFas), the apoptotic cell death pathway is induced by clustering of Fas caused by agonistic anti-Fas antibodies [21].

2.1. Time-lapse microscopy

Time-lapse imaging is a technique that specifies a predefined delay between acquisition of images. This technique allows monitoring of morphological changes in individual cells in a dynamic and comparative manner and reveals differences between apoptosis and necrosis. Time-lapse images can be recorded by using differential interference contrast (DIC) optics either alone or in combination with epifluorescence microscopy.

The time-lapse microscope used in this study consists of a Leica ASMDW live cell imaging system (Leica Microsystems, Mannheim, Germany), which includes a DM IRE2 microscope equipped with an HCX PL APO 63×/1.3 glycerin corrected 37 °C objective and a 12 bit Coolsnap HQ Camera. The microscope contains a temperature and CO_2 controlled incubator chamber.

2.1.1. Differential interference contrast (DIC) microscopy

The DIC optics create a virtual relief image that allows morphological analysis of transparent objects. Using DIC mode the following parameters can be analyzed: (1) morphological changes that are specific for apoptosis or necrosis; (2) the duration and order of onset of subcellular events, such as rounding up of cells, formation of apoptotic bodies, and formation of balloon-like structures.

2.1.1.1. Sample preparation. For time-lapse microscopy, the cells (4×10^3 cells per chamber) were seeded two days before analysis in an 8-chambered cover glass (Lab-Tek® Chambered #1.0 Borosilicate Cover Glass System, Nunc) to allow the cells to attach to the bottom and become flattened so that a better morphological profile can be obtained. Then cell death was induced. For example, necrosis and apoptosis can be induced in L929sAhFas cells by TNF (1000 IU/ml) and agonistic anti-Fas antibody (BioCheck GmbH, anti-Fas, 125 ng/ml), respectively. Recombinant human TNF was produced in *Escherichia coli* and purified to at least 99% homogeneity. The specific biological activity was 2.3×10^7 IU/mg as determined in a standardized cytotoxicity assay on L929sA cells. Immediately after adding cell death stimuli, place the chambered

cover glass in the time-lapse microscope. The cells are imaged using 3 D (x, y and z) time-lapse microscopy with DIC optics.

Apoptosis is characterized by rounding up of the cells, blebbing, and formation of apoptotic bodies, which culminates in formation of a balloon-like structure, indicating the loss of plasma membrane integrity and development of secondary necrosis. In contrast, cellular swelling and formation of a balloon-like structure characterize necrosis. These distinct morphological features of apoptotic versus necrotic cell death can be viewed in time-lapse movies of L929sAhFas cells (apoptosis morphology.avi; necrosis morphology.avi).

2.1.2. Combination of differential interference contrast (DIC) and epifluorescence microscopy

Combination of DIC with epifluorescence mode allows the use of fluorescent probes and makes it possible to link specific morphological features of cell death with particular molecular or subcellular cell death events. Many fluorescent probes are available from Invitrogen, including propidium iodide (PI) or Sytox green (to determine plasma membrane permeability), Annexin V-Alexa Fluor 488 (to monitor phosphatidylserine exposure), LysoTracker (to visualize lysosomal integrity), tetramethylrosamine (TMRM) (to measure mitochondrial depolarization), and carboxy-H_2DCFDA (to detect production of reactive oxygen species).

2.1.2.1. Sample preparation. Cells are seeded as described above for DIC mode. To monitor morphological changes and membrane permeability in parallel, PI was added to a final concentration of 3 μM simultaneously with the cell death stimuli. PI is a fluorescent membrane-impermeant dye that stains the nuclei by intercalating between the stacked bases of nucleic acid. Since PI enters the cell only if the cell membrane becomes permeable, it is widely used in cell death research to measure the integrity of the plasma membrane. When bound to nucleic acids, the absorption maximum for PI is 535 nm and the fluorescence emission maximum is 617 nm. Three-dimensional time-lapse microscopy was performed using a combination of DIC and epifluorescence optics. The amount of light to which the cells are exposed should be optimized for each cell type and for each fluorescent probe in order to reduce phototoxicity and photobleaching, so that no cell death is observed in control conditions without stimuli. This means low exposure times, low lamp voltage, a small number of z-sections and time frames, and binning of pixels on the CCD camera. Binning allows charges from adjacent pixels to be combined, which allows shorter exposure times. The advantage of this technique is that you need shorter exposure times because sensitivity increases with the binning factor, which translates into reduced phototoxicity, although at the expense of reduced spatial resolution.

Staining of the nucleus with PI allows discrimination between primary and secondary necrosis. Because secondary necrotic cells had already passed through an apoptotic stage, their nuclei are fragmented and/or condensed. Moreover, the DNA had undergone internucleosomal cleavage and chromatin structure is lost, and so nuclei stain homogenously with PI. Necrotic cells have uncondensed nuclei with prominent nucleoli. The distinct pattern of PI staining of apoptotic and necrotic L929sAhFas cells can be viewed in time-lapse movies (apoptosis_PI.avi and necrosis_PI.avi).

2.2. Flow fluorocytometry

The different morphologies of apoptotic and necrotic cells can also be detected by analyzing their light-scattering properties in flow fluorocytometry. The forward scatter is commonly used to approximate cell size, which permits distinction of apoptotic blebs from apoptotic cells. The amount of side scatter of laser light generally correlates with the degree of granularity of a cell. A typical FACS Calibur flow fluorocytometer (Becton Dickinson) can analyze at least five different parameters: (I) forward scattered light (FSC, indicates cell size), (II) side scattered light (SSC, indicates granularity), (III) FL1 (green fluorescence; used for FITC, R123, GFP), (IV) FL2 (red fluorescence; used for PI, CMTMros, PE), and (V) FL3 (far red fluorescence, used for PI, Cy-Chrome). Cell size and granularity can be studied in combination with markers of membrane integrity. For example, PI is excited with a xenon or mercury-arc lamp or with the 488 line of an argon-ion laser and can be detected in the FL2 or FL3 channel of a flow fluorocytometer (FACSCalibur flow fluorocytometer, Becton Dickinson). PI has a broad emission spectrum, which is problematic if it is used in combination with other fluorochromes. Only fluorochromes with a clearly distinct emission spectrum or with only a small emission spectrum overlap can be used. A small emission overlap can be compensated during flow fluorocytometric measurements by changing the detector or amplifier gain of any of the fluorescence parameters (FL1, FL2 or FL3). To check or adjust the compensation, control samples labeled singly with each color are used, as well as unlabeled samples. Data are typically stored in computer memory, which permits the reanalysis of the data after collection.

2.2.1. Sample preparation

Flow fluorocytometry of adherent cell lines requires detachment of the cells from the culture flask or plate. In order to work faster during kinetics and to avoid interfering manipulations, such as trypsin and EDTA treatment, which could lead to damage or permeabilization of the cells, it is advisable when doing FACS analysis to grow adherent cells in suspension. Importantly, the ability of the adherent cells to grow in suspension should be tested beforehand. Cells were seeded at 1.5×10^5 cells/ml per well the day before analysis in uncoated 24-well suspension plates (Sarstedt) to avoid attachment of the cells to the bottom. The next day apoptotic or necrotic cell death was induced. Cell samples from suspension cultures were ana-

lyzed at regular intervals on the flow fluorocytometer. For this a volume of 270 μl of cells from the 24-well suspension plate was transferred to a 5-ml polypropylene round bottom tube, and 30 μl of PI was added from a 10× solution prepared from a 3 mM stock. It is important to stress that secondary necrosis is the end stage of apoptosis, and that it displays the same features as necrotic cells, such as loss of membrane integrity and leakage of proteins in the supernatant [8]. It is advisable to perform kinetics studies to detect the different features of apoptotic and necrotic cells (discussed later). The flow fluorocytometer was set up for a dot plot with forward and sideward scatters both on a linear scale to determine cell size and granularity (Fig. 1). PI was detected in FL3 channel at 610 nm, e.g. on a FAC-

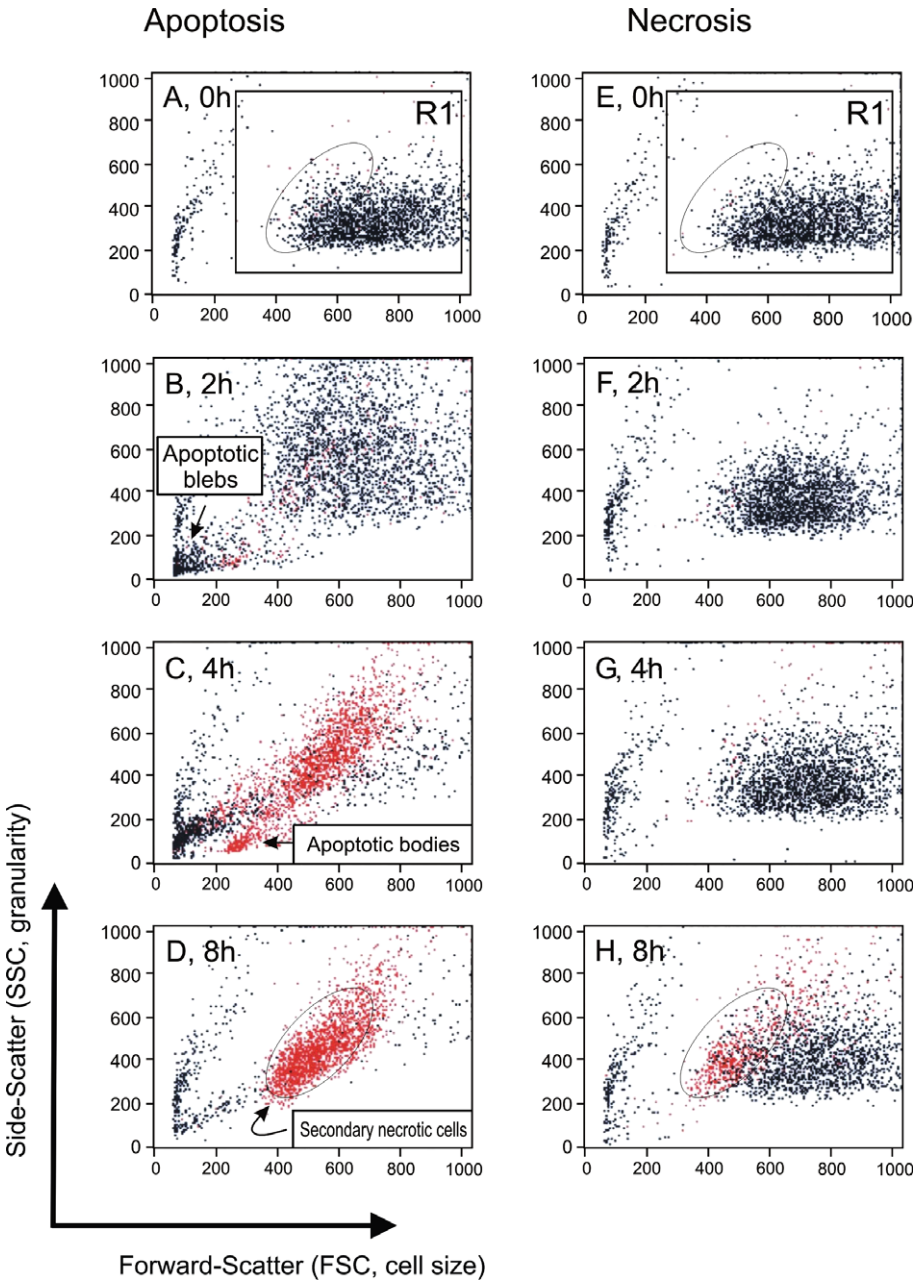

Fig. 1. Analysis of cell morphology versus cell permeability by flow fluorocytometry. Cells were analyzed by flow fluorocytometry for changes in size (forward scatter) and granularity (side scatter), as well as for loss of membrane integrity by using propidium iodide uptake (FL3). At time point zero the viable cell population, which consisted mainly of PI-negative cells, was detected within the region of analysis. After 2 h of apoptosis induction by anti-Fas antibodies, L929sAhFas cells exhibited blebbing (A–D), which caused increased diffraction of the laser beam, as manifested in spreading of the dots (B). The release of apoptotic particles is detected by the appearance of a population of small PI-negative dots (the absence of DNA) in the lower left corner of the dot plot (B). Condensation of the nucleus, shrinkage of the cells and formation of apoptotic bodies containing DNA is represented by the population of PI-positive red dots in the lower left corner on the dot plot (C). The population of secondary necrotic cells (D) clearly co-localized with the population of primary necrotic cells (H). The time at which PI-positive cells appeared is indicated in red on the dot plots. (For interpretation of the references to color in this figure legend, the reader is referred to the web version of this paper.)

SCalibur flow fluorocytometer (Becton Dickinson) equipped with a water-cooled argon-ion laser at 488 nm. To clearly see the dead cells on the dot plot, PI-positive cells are gated, e.g. in red, in the FL3 histogram. The region of analysis was gated (R1), and gating must be large enough in order to measure both living and dying cell populations.

2.3. Transmission electron microscopy

Transmission electron microscopic (TEM) analysis has been considered a 'golden standard' in cell death research. It provides two- and three-dimensional (using Fourier methods) images of the inside of cells, which makes it possible to understand biological structure–function relationships at cellular, subcellular and molecular levels [22,23]. Although TEM is time consuming and requires more expensive equipment, it offers much higher resolving power (0.1–0.4 nm), thereby providing much more detailed information about cell morphology. TEM is considered the most accurate method for distinguishing apoptosis from necrosis in cell cultures. However, preparation of dying cells for electron microscopy may be difficult because dying cells typically detach from their substrate, and spinning down these floating cells may cause damage to their original morphology. Below we suggest a method that helps to circumvent this problem by using macrophages attached to the bottom of tissue culture plates to capture dying apoptotic and necrotic cells. The samples were viewed with a Jeol 1200 EXII TEM at an accelerating voltage of 80 kV.

2.3.1. Sample preparation

Macrophages were seeded in adherent 6-well plates at 5×10^5 cells per well and target cells in uncoated 6-well suspension plates at 5×10^5 cells per well. The target cells were grown in suspension plates so that the population of dying cells could be transferred easily to the well containing attached macrophages. Apoptosis and necrosis were induced in target L929sAhFas cells either by agonistic anti-Fas antibody (250 ng/ml, for at least 1 h) or mTNF (10,000 IU/ml, for at least 7 h), respectively. The choice of time points depend on the kinetics of cell death and have to be optimized for each cell line and death inducer. A coculture of macrophages with target cells was established in a 1:1 ratio and incubated for at least 1 h. After that, cocultures of macrophages and target cells were fixed overnight at 4 °C in the 6-well plate by immersion in TEM fixation buffer (2% glutaraldehyde containing 1 mM $CaCl_2$ and 0.1 M sucrose buffered with 0.1 M Na-cacodylate, pH 7.4). Following several rinses in 100 mM Na-cacodylate containing 7.5% w/v sucrose, the samples were post-fixed overnight at 4 °C in 1% w/v OsO_4 in the same buffer (without sucrose). They were then washed several times in 100 mM Na-cacodylate containing 7.5% w/v sucrose and dehydrated in a graded series of ethanol (50% for 15 min, 70% for 20 min, 90% for 30 min and 100% for 90 min). Following infiltration with 100% ethanol, they were infiltrated with a mixture of ethanol and LX-112 resin (Ladd Research Industries, USA) as follows: 1:1 for 30 min and 1:2 for 30 min. It was finally infiltrated with 100% resin for 120 min, and then polymerized for at least 48 h at 60 °C. Finally, the plastic was broken off of the polymerized block, sawed into pieces to fit the ultramicrotome holders, and ultra thin sections of 60 nm were mounted on formvar-coated 100-mesh copper grids. The samples were evaporated in a JEOL (JEC-530) autocarbocoater at 4 V for 3 s and then stained with uranyl acetate (7.5% in bi-distilled water, 1 drop per grid for 20 min) and Reynold's lead citrate (1 drop per grid for 10 min). The semi-thin sections were examined by TEM.

Two of the earliest classic ultrastructural changes detectable in apoptosis are formation of uniformly dense masses of chromatin distributed against the nuclear envelope [24] and persistence of a nucleolar structure until the very late stages [25]. Apoptotic cells (Fig. 2B) are typically characterized by the loss of specialized surface structures, such as microvilli and cell–cell contacts, condensation of cytoplasm, and formation of membrane-bound apoptotic

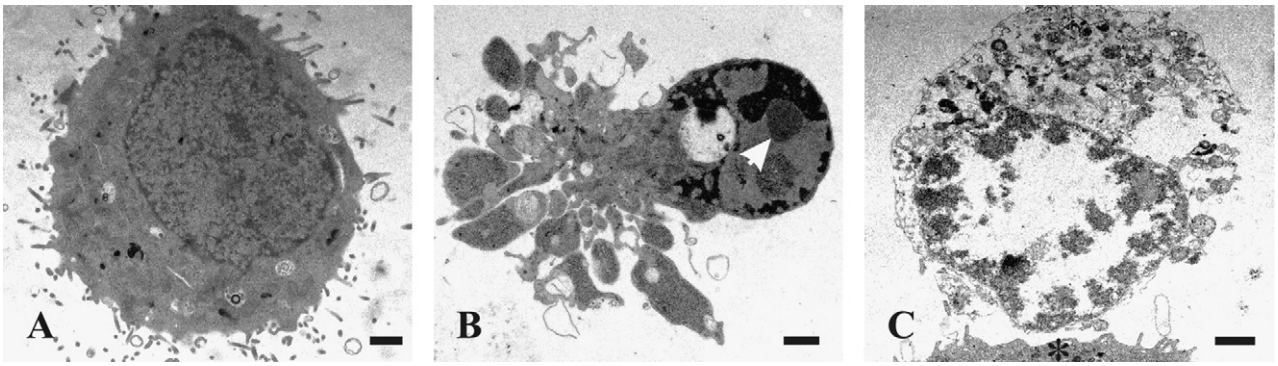

Fig. 2. Analysis of cell morphology of apoptotic and necrotic cells by transmission electron microscopy. Unstimulated L929sAhFas fibrosarcoma cell (A) and cells exposed either to agonistic anti-Fas for 1 h (B) or to hTNF for 7 h (C). (A) The cell shows microvilli protruding from the entire surface, a smoothly outlined nucleus with chromatin in the form of heterochromatin and well-preserved cytoplasmic organelles. (B) Apoptotic cell with sharply delineated masses of condensed chromatin, convolution of the cellular surface and formation of apoptotic bodies. Note the nucleolus (arrow head) near a cup-shaped chromatin margination. (C) Necrotic cell near the macrophage (asterisk) with clumps of chromatin with ill-defined edges, swollen mitochondria and loss of plasma membrane integrity. Scale, bars: 1 μm.

bodies of different sizes containing well-preserved but compacted cytoplasmic organelles and/or nuclear fragments [24,26]. Necrosis is morphologically distinct from apoptosis and is characterized by a general swelling of the cell (oncosis) and of the cytoplasmic organelles, and rapid loss of plasma membrane integrity (Fig. 2C). Remarkably, nuclear morphology remains relatively unchanged until later stages, when chromatin condenses into small irregular pieces [27].

3. Methods for analysis of cell surface markers

Phosphatidylserine (PS) is an aminophospholipid that resides in the inner leaflet of the plasma membrane of living cells. During apoptotic cell death, PS is actively externalized to the outer surface of the plasma membrane, where its presence is required for recognition and engulfment of dying cells [2]. Several possible mechanisms for PS exposure have been proposed, including a coordinate increase in phospholipid flip–flop due to inactivation of the aminophospholipid translocase; flip refers to inward and flop to outward movement [28]. Recently, a new mechanism of PS exposure has been discovered in *Caenorhabditis elegans* [29]. These workers identified a *tat*-1 gene that might encode an aminophospholipid transporter, because knocking down this gene abrogated PS exposure on apoptotic cells and reduced clearance of dead cell corpses.

PS is an early marker of apoptotic cells death. It can be detected by using annexin V, a Ca^{2+}-dependent phospholipid-biding protein, conjugated with various fluorochromes, such as fluorescein isothiocyanate, FP488, Alexa Fluor dyes, phycoerythin and carbocyanines. Green fluorescent annexin V (Alexa Fluor 488-conjugated Annexin V) is the most widely used target-specific probe for measuring PS exposure. Combining annexin V Alexa Fluor with PI can help to distinguish between apoptosis and necrosis [30]. During apoptosis, there is a lag period between PS positivity and PI positivity, while in necrotic cells both events coincide. However, it is important to mention that in some cellular systems necrotic cells, while remaining PI negative, also externalize PS [31]. The reason for this is not clear, but weaker necrotic signaling probably favors the detection of PS exposure with absence of rapid membrane permeabilization (Krysko and Vandenabeele, unpublished observations). Thus PS^+/PI^- staining might not discriminate between apoptosis and necrosis in some cases, and for that reason more than one cell death marker should be used to characterize cell death types. This approach is discussed in Section 3.1. We would like to point out that PS exposure on dying cells could also be detected *in vivo*. Annexin V and its derivatives, labeled with ^{123}I, ^{125}I, ^{124}I, ^{18}F and ^{99m}Tc, are used in a broad range of imaging applications in apoptosis research, such as single-photon emission computed tomography, autoradiography and positron emission tomography [32,33].

Below we describe an assay that measures cell membrane permeability and phosphatidylserine (PS) exposure by flow fluorocytometry, for the purpose of discriminating apoptosis from necrosis Fig. 3.

3.1. Analysis of PS exposure versus cell permeability by flow fluorocytometry (FACS)

Measurement of cell death by using Annexin V may be substantially affected by calcium concentration, time of incubation on ice, and type of medium [34]. Therefore, the lowest possible concentration of calcium should be used, usually not exceeding 1.8 mM, and it must be added only 10 min before analysis. Moreover, the binding buffer should be a simple balanced salt solution containing Na, K, Cl, and Mg; HEPES-based buffers should be used, rather than phosphate buffers [34]. For time-lapse applications the assay can also be done in cell culture medium. Measurements in RPMI 1640 medium are not recommended because of the relatively high concentration of phosphate and low concentration of Ca^{2+}. DMEM and Medium 199 satisfy the PS-binding conditions of annexin V-Alexa and so they can be used for real-time imaging.

3.1.1. Cell preparation

In order to analyze on flow fluorocytometry PS-exposure versus cell permeability, L929sAhFas cells were seeded as described in Section 2.2. The next day, the cells were stimulated with TNF (1000 IU/ml) or anti-Fas (125 ng/ml) and analyzed at regular intervals on a flow fluorocytometer. For this, $1.5–3 \times 10^5$ cells were transferred to an Eppendorf tube, centrifuged for 5 min at 250*g* at 4 °C, and resuspended in 1 ml ice-cold Annexin V-binding buffer (10 mM HEPES NaOH, pH 7.4, 150 mM NaCl, 5 mM KCl, 1 mM $MgCl_2$ and 1.8 mM $CaCl_2$). Cells were kept on ice to stop further biochemical activity within the cells. Then the cells were centrifuged for 5 min at 250*g* at 4 °C and resuspended in 270 μl of Annexin V-binding buffer containing 1 μg/ml of Annexin V-Alexa Fluor 488. After incubation for 5 min on ice in the dark, and just before flow fluorocytometric analysis, 30 μl of PI from a 10× solution (prepared from a 3 mM PI stock) was added to the cell suspension. The samples were analyzed by generating a dot plot showing Annexin V-Alexa (FL1) versus PI (FL3), and defining quadrants that divide cell populations according to Annexin V and PI positivity. Single-stained cells should be included in the experiment to set up compensation and quadrant markers, i.e. cells stained only with Annexin V-Alexa (no PI added) and cells stained only with PI (no Annexin V-Alexa added). The absorption maximum for Anexin V-Alexa Fluor is 495 nm, and its fluorescence emission maximum is 519 nm. PI bound to nucleic acids has absorption and fluorescence emission maxima of 535 nm and 617 nm, respectively. FL1 (520 nm) and FL3 (610 nm) channels detect Annexin-V-Alexa staining and PI uptake, respectively, on a FACSCalibur flow fluorocytometer (Becton

Dickinson) equipped with a water-cooled argon-ion laser at 488 nm. The dynamics and interrelation between PS exposure and PI permeability during apoptosis and necrosis in L929sAhFas cells can be seen on time-lapse movies (apoptosis_PS_PI.avi and necrosis_PS_PI.avi).

4. Methods for analysis of intracellular markers

In this section we will describe the use of intracellular markers, such as fragmentation of DNA, activation of caspases, cleavage of Bid into its truncated pro-apoptotic form (tBid), and release of cytochrome *c*; all these can help distinguish between apoptosis and necrosis. None of these events occurs in TNFR1-induced necrotic cell death [8]. In addition to determining the activation pattern of different caspases, the cleavage pattern of a variety of substrates, such as PARP and ICAD, can also be examined [35]. It is important to stress that measuring mitochondrial membrane potential (TMRM, rhodamine123, JC-1, Molecular Probes) or ROS production (dihydrorhodamine123) does not distinguish the mode of cell death [36,37] and therefore are not described in this review. In both cell death pathways the membrane potential of the mitochondria drops and the cells start producing ROS [8,38].

4.1. Analysis of DNA fragmentation by flow fluorocytometry (FACS)

What most distinguishes apoptosis from necrosis is DNA fragmentation and formation of high molecular weight (>50 kbp) and nucleosome-sized (200 bp) DNA fragments [39,40]. There are several biochemical techniques based on agarose gel electrophoresis for detection of DNA ladders [41]. However, these techniques are time consuming. We describe an easy and quantitative way to analyze DNA fragmentation based on flow fluorocytometric detection of DNA hypoploidy after adding PI to the dying cells and permeabilizing them by freeze-thawing. PI intercalates in the DNA and the size of DNA fragments appears as a hypoploid DNA histogram. This technique allows discrimination between apoptotic and necrotic cell death.

Cell preparation. After seeding the cells and inducing cell death as described in Section 2.2, 270 μl of cells were transferred in suspension from the 24-well plate to a 5-ml polypropylene round bottom tube and combined with 30 μl of 10× PI solution prepared from a 3-mM stock. The tubes were freeze-thawed once by placing them briefly in liquid nitrogen. This procedure permeabilizes the cells and stains them with PI. The samples were then analyzed by flow fluorocytometry (Fig. 4). The experimental setup was the same as the one described in Section 2.2.

4.2. Analysis of caspase activation

Caspases are a family of cysteine aspartate-specific proteases. They are synthesized as zymogens, and they consist of a prodomain of variable length, followed by a p20 and a p10 unit that contain the residues essential for substrate recognition and catalytic activity. They are activated either by proximity-induced auto-proteolysis by interacting with a platform of adaptor proteins through a protein interaction motif in the prodomain (DED, death effector domain; or CARD, caspase recruitment domain), or by cleavage by upstream proteases in an intracellular cascade. These proteolytic activities lead to separation of the prodomain from the p20 and p10 subunits, which then form an active heterotetramer [35]. In the following sections we will describe how caspase activity could be investigated by western blotting and by the use of fluorogenic substrates.

4.2.1. Western blot

4.2.1.1. Sample preparation. On day zero, 6×10^5 cells per well are seeded in 6-well suspension tissue culture plates. The next day the cells are stimulated and collected in 1.5-ml Eppendorf tubes at regular time intervals. Then the cell suspension is centrifuged for 5 min at 250*g*, medium is aspirated, the cells are washed with 1 ml of cold PBS, centrifuged again, and the PBS is aspirated. The cells are lysed in 150 μl of cold caspase lysis buffer and kept on ice to stop further biochemical activity, or else they can be frozen before analysis. Cell lysis and processing should be standardized with respect to volumes and to the number of seeded cells, and no correction should be applied to protein content because in the later stages of cell death the cells start to leak cytosolic proteins in the supernatant (discussed later). After lysis, cell debris is removed by centrifugation for 10 min at 20,800*g* at 4 °C, the remaining cytosol is transferred to another Eppendorf tube, 0.2 volume of 5× Laemmli buffer is added, and the mixture is boiled for 5–10 min. Laemmli-buffer 5× contains 312.5 mM Tris–HCl, pH 6.8, 10% SDS, 50% glycerol and 20% β-mercapto-ethanol. Equal volumes are loaded on 12.5% SDS–polyacrylamide gels, and after separation the proteins are transferred to a nitrocellulose membrane. The different caspases are detected with the appropriate antibodies: anti-human caspase-3 (BioSource) and anti-human caspase-7 (StressGen Biotechnologies Corporation). The signal is revealed with Chemiluminescence Reagent Plus (PerkinElmer Life Sciences, Boston, USA).

Activation of initiator procaspases results in the appearance of a prodomain, and p20 and p10 subunits. Proteolytic activation of effector procaspases leads eventually to the appearance of a typical p20 and p10 subunits. Depending on the antibody used, one or all proteolytic fragments can be detected. There are also antibodies that specifically recognize the activated forms of caspases (PharMingen). It is important to mention that activated caspase-3 could also be detected *in situ* by immunohistochemistry to discriminate between apoptosis and necrosis (antibodies available from companies such as Cell Signaling Technology) [42].

When apoptosis was induced by anti-Fas, the activation of caspase-3 and -7 was characterized by the appearance of the p20 subunit [8]. In contrast, in necrosis,

which is induced by stimulation of TNFR1, p30 caspase-3 and -7 are not activated and thus a p20 subunit does not appear [8]. Procaspases and activated caspases are also released from primary and secondary necrotic cells, respectively, and can be detected in their supernatants (see Section 5.2.).

4.2.2. Fluorometry

To measure the activity of caspases instead of their proteolytic activation state, one can use fluorogenic substrates for caspases. These substrates contain the minimal amino acid composition corresponding to the cleavage site of a typical substrate coupled to 7-amino-4-methylcoumarin (AMC) or 7-amino-4-trifluoromethylcoumarin (AFC). Hydrolysis of the peptide substrate releases free AMC or AFC, the fluorescence of which can be measured in a fluorometer.

The first synthetic substrates designed and used to measure and analyze caspase activities were based on the cleavage sites of the initial cellular protein substrates that were identified [35,43]. They usually consisted of a tetrapeptide with aspartate at position P1 (XXXD) conjugated to a fluorogenic AMC or AFC. In this way acetyl(Ac)-DEVD-AMC was identified as a preferred substrate for caspase-3 and -7, Ac-LEHD-AMC for caspase-5, Ac-YVAD-AMC for caspase-1 and -4, Ac-IETD-AMC for caspase-8 and -6, and Ac-WEHD-AMC for caspase-1, -4 and -5 [35]. The specificity of the substrates is not always restricted to those mentioned by the manufactures [44]. The problem is that substrate specificity is lost outside a certain range of caspase concentration. High concentrations of caspase-3 will also cleave Ac-IETD-AMC, the caspase-8 and -6 substrate. Therefore, enzymatic measurements of caspase activities should be combined with western blotting to identify the presence and activation status of the caspase (see Section 4.2.1). In addition, active caspases and procaspases are released from primary or secondary cells and can be detected in their supernatants (see Section 5.2).

4.2.2.1. Sample preparation. The cells are seeded and processed as described in Section 4.2.1. After centrifuging the cells for 5 min at 250*g* and removing the PBS, the cells are lysed in 150 μl cold caspase lysis buffer (1% NP-40, 10 mM Tris–HCl, pH 7.4, 10 mM NaCl, 3 mM $MgCl_2$). The following protease inhibitors should be added to caspase lysis buffer directly before cell lysis: 1 mM PMSF, 0.3 mM aprotinin, and 1 mM leupeptin. Pefablock protease inhibitors or other total protease inhibitor mixes should not be used because they interfere with caspase activity. In order to block the catalytic cysteine of caspases, 1 mM of oxidized glutathione (GS–SG) is added to prevent the activation of caspase cascades during lysis, which is carried out on ice to stop further biochemical activity. At this stage the samples can be frozen for storage. Importantly, before measurement of caspase activity in CSF buffer, 10 mM dithiothreitol is added to remove the GSH from the catalytic cysteine. Next the cell debris is removed by centrifuging the lysate for 10 min at 20,800*g* (4 °C) and the cytosol is transferred to another Eppendorf tube (cytosolic cell lysate). Caspase activity is measured by incubating 10 μg cytosolic cell lysate with 50 μM of the fluorogenic substrate, e.g. Ac-DEVD-AMC, in 150 μl CFS-buffer. Dithiothreitol (DTT) is added to a final concentration of 10 mM. Caspase fluorogenic substrates are prepared as 100 mM stock solution in DMSO: Ac-DEVD-AMC, Ac-LEHD-AMC, Ac-YVAD-AMC, Ac-IETD-AMC and Ac-WEHD-AMC (Peptide Institute, Osaka, Japan). The release of fluorescent AMC is monitored every 2 min for 1 h in a fluorometer at 37 °C (e.g. CytoFluor, PerSeptive Biosystems), using a filter with an excitation wavelength of 360 nm and another with an emission wavelength of 460 nm. The data are expressed as the time-rate of increase in fluorescence (Δfluorescence/min) [8,45]. Note that caspase activity is only detected in apoptotic conditions. CSF buffer: 10 mM HEPES NaOH, pH 7.4, 220 mM mannitol, 68 mM sucrose, 2 mM $MgCl_2$, 2 mM NaCl, 2.5 mM H_2KPO_4, 0.5 mM EGTA, 0.5 mM sodium pyruvate and 0.5 mM L-glutamine. PBS: 8 g/L NaCl, 0.2 g/L KCl, 2.89 g/L $Na_2HPO_4{\cdot}12H_2O$ and 0.2 g/L KH_2PO_4.

4.3. Analysis of Bid cleavage and cytochrome c release by western blotting

To determine the role of the mitochondrial apoptotic pathway, one can investigate the engagement of the mitochondria at the different stages: Bid proteolytic activation, tBid translocation and cytochrome *c* release. In order to detect the release of cytochrome *c* in the cytosol, the organelle and cytosolic fractions should be separated without causing release of cytochrome *c* from the mitochondria as an artifacts of organelle preparation. It is advisable to use a mild detergent, digitonin, at a concentration of 0.02%, which permeabilizes the plasma membrane but leaves the mitochondria and lysosomes intact. The concentration of digitonin and the required lysis period has to be optimized for each cell type. Serial concentrations of digitonin should be tested to select the condition in which the outer membrane is permeabilized (detection of cytosolic proteins, e.g. actin), while the mitochondrial or lysosomal membranes remain intact (no detection of mitochondrial proteins, e.g. COX, or lysosomal proteins, e.g. hexosaminidase).

4.3.1. Sample preparation

The cells are seeded as described in Section 4.2.1. After centrifugation for 5 min at 250*g* and removing PBS, the cells are lysed in 100 μl of 0.02% digitonin dissolved in CFS buffer and left on ice for 1 min to stop biochemical activity. Then the lysate is centrifuged for 10 min at 20,800*g* (4 °C) and the cytosol is transferred to an Eppendorf tube. One-fifth volume of 5× Laemmli buffer is added to the cytosolic lysate and 100 μl 1× Laemmli buffer to the remaining organelle fraction. The samples are boiled for 5–10 min and equal volumes of the organelle fraction or cytosolic cell lysate are loaded per lane on 12.5% SDS–poly-

acrylamide gels. After electroblotting the proteins to a nitrocellulose membrane, detect Bid cleavage and cytochrome *c* with appropriate antibodies from R&D Systems and Pharmingen, respectively. Reveal the signal with Chemiluminescence Reagent Plus (PerkinElmer Life Sciences, Boston, USA).

Induction of apoptosis by anti-Fas antibodies leads to early cleavage of full length Bid into its pro-apoptotic truncated form (tBid). tBid can be detected in the cytosolic fraction only briefly and in small amounts. Most of tBid becomes rapidly associated with the organelle fraction. To accurately detect the engagement of Bid, it is advisable to analyze both the disappearance of Bid from the cytosol and the appearance of tBid in the organelle fraction. In necrotic cells, no cleavage of p22 Bid is detectable either in the cytosol or in the organelle fraction. During the late stages of necrosis, Bid disappears from the cytosol due to leakage and a small amount of tBid becomes detectable in the organelle fraction, probably due to alternative Bid cleavage by lysosomal proteases [46]. Remarkably, the appearance of tBid in the organelle fraction during anti-Fas induced apoptosis coincides with the release of cytochrome *c* into the cytosol. During secondary necrosis of anti-Fas-stimulated cells, cytochrome *c* also accumulates in the culture supernatant. TNFR1-induced necrosis does not result in detectable release of cytochrome *c* in the cytosol. However, in the late necrotic phase of TNF-stimulated cells, cytochrome *c* accumulates in the culture supernatant from the moment that the plasma membrane loses its integrity. Representative western blots of tBid cleavage and cytochrome *c* release can be found in the article of Denecker et al. [8].

5. Methods for analysis of extracellular markers

If apoptotic cells are not taken up by phagocytosis, they become secondary necrotic cells with many features of primary necrotic cells (discussed in Section 3.1). For example, the plasma membrane becomes permeabilized, with consequent leakage of large amounts of intracellular contents, which have many biological effects, e.g. induction of immune responses and chemoattraction of antigen presenting cells [47]. Detection of lactate dehydrogenase (LDH) release may provide an easy method for determining the extent of cell death irrespective of the type of cell death, as discussed below. However, the detection in the supernatant of certain factors released either from primary or from secondary necrotic cells may be instrumental for characterizing these cell death types. In this section we will describe the detection of caspases-3 and -7, a high mobility group box 1 protein (HMGB-1), and cytokeratin 18 (CK18) in the supernatant of primary or secondary necrotic cells.

5.1. Analysis of lactate dehydrogenase release

LDH is a cytosolic enzyme present in all mammalian cells. The plasma membrane is impermeable to LDH, and loss of its integrity is detectable by the release of LDH into the supernatant [48], where its enzymatic activity can be measured. *In vitro* release of LDH from cells provides an accurate measure of cell membrane integrity and cell viability irrespective of the type of cell death. This method allows large-scale screening of conditions to be carried out in 96-well plates, or optimization of concentrations of inhibitors or sensitizing reagents. LDH activity in the culture medium can be measured by the CytoTox 96 Assay, which is based on a coupled two-step reaction. In the first step, LDH catalyzes the reduction of NAD^+ to NADH and H^+ by oxidation of lactate to pyruvate. In the second step of the reaction, diaphorase uses the newly-formed NADH and H^+ to catalyze the reduction of a tetrazolium salt [2-*p*-(iodophenyl)-3-(*p*-nitrophenyl)-5-phenyltetrazolium chloride, INT] to highly-colored formazan, which absorbs strongly at 490–520 nm. The amount of formazan formed is proportional to the amount of LDH released into the culture medium.

Sample preparation. The cells are seeded the day before analysis at 2×10^4 cells in 100 μl per well in 96-well plates. After induction of cell death, 50 μl of cell supernatant is placed in a 96-well plate. Following addition of 50 μl of reconstituted substrate mixture (CytoTox 96™ Assay, Promega) and incubation for 30 min at room temperature, 50 μl of stop solution is added to each well and optical density at 492 nm is measured. Results are expressed either as optical absorbance values, or converted to international units of enzyme with reference to a standard curve obtained with the positive LDH control provided with the CytoTox 96™ assay.

5.2. Analysis of caspase release

Secondary necrosis is characterized by the release into the culture medium of the p20 subunits of caspases-3 and -7, whereas in necrosis this does not occur and only procaspases-3 and -7 can be detected in the supernatant [8]. Therefore, detection of p20 subunit of caspases-3 and -7 in the supernatant may be indicative of apoptotic cell death. Fluorogenic substrates (discussed in Section 4.2.2) can also be used to detect caspase release into the supernatant. It is important to stress that secondary necrosis is distinguished from primary necrosis by detection of caspase-3 and -7 activity in the supernatant. In the late stages of necrosis no active caspase-3 and -7 can be observed in the supernatant [8]. In the following sections we will describe how caspase activity in the supernatant of dying cells can be investigated by western blotting and by the use of fluorogenic substrates.

5.2.1. Western blotting

5.2.1.1. Sample preparation. On day zero, 1.2×10^6 cells are seeded per well in a 90-mm Petri dish. The next day the cells are washed twice with serum-free medium and cell death is induced after resuspending the cells in 7 ml of serum-free medium. Supernatant samples are then collected at regular time intervals in 15-ml tubes and centrifuged for 5 min at 250*g*. Five milliliters of the

supernatant is transferred to new 15-ml tubes. Following centrifugation, 4 ml of supernatant is divided into 1.5-ml Eppendorf tubes, and 0.1 volume of deoxycholate is added in each tube from a stock of 5 mg/ml. Deoxycholic acid is added in base form (sodium salt), and it precipitates after addition of the stronger trichloroacetic acid. In this protocol, it acts as a co-precipitant and helps the protein to precipitate. These samples are then incubated on ice for 20 min, 0.1 volume of 100% trichloroacetic acid (Sigma) is added to each tube, and the tubes are incubated on ice for 30 min. After that, the samples are centrifuged at 20,800*g* for 5 min at 4 °C, the supernatant is removed, and 500 μl of ice-cold 100% acetone is added. Following centrifugation at 20,800*g* for 5 min at 4 °C, the pellet is dissolved in 20–30 μl of sample buffer (3 volumes of 2× Laemmli buffer + 1 volume of 1 M Tris–HCl), and the samples are pooled. If the Laemmli buffer turns yellow, 1 M Tris–HCl buffer is added 1 μl at a time until it turns blue. The samples are boiled for 10 min and caspase activation is analyzed by western blotting as described in Section 4.2.1.

Onset of apoptosis is characterized by activation of caspase-3 and -7, which is detectable in the cytosolic fraction (see Section 4.2.1). Upon disruption of plasma membrane integrity and development of secondary necrosis, active caspase-3 and -7 become detectable in the supernatant. In contrast, in the late stages of necrosis no active caspase-3 and -7 can be observed in the supernatant [8].

5.2.2. Fluorometry

Sample preparation. The cells are seeded the day before analysis at 2×10^4/100 μl per well in 96-well plates. The cells are exposed to a serial dilution of a cell death stimulus, and caspase activity is measured by incubating at least 20 μl of supernatant with 50 μM of the fluorogenic substrate, e.g. Ac-DEVD-AMC, in 150 μl CFS buffer, as described in Section 4.2.2.

5.3. Analysis of HMGB-1 release by western blotting

The high mobility group box 1 protein (HMGB-1) is another protein that is released only from necrotic cells but remains bound in apoptotic cells even when they are undergoing secondary necrosis [49]. HMGB-1 acts as an architectural chromatin-binding factor that bends DNA and promotes protein assembly on specific DNA targets [49]. Once released from necrotic cells, HMGB-1 has a broad range of biological functions, such as activation of macrophages through TLR2 and TLR4 [50] and chemoattraction and activation of dendritic cells (DCs) [51]. It is also required for processing and presentation of tumor antigens by DCs [52]. Release of HMGB-1 is detected by western blotting.

5.4. Analysis of cytokeratin 18 release by ELISA

In live epithelial cells, cytokeratins are insoluble because they are complexed in intermediate filaments [53]. However, during cell death CK18 is released and can be detected in the supernatant. Remarkably, the fate of epithelial-specific intermediate filament cytokeratin (CK18) depends on the type of cell death. The M30-Apoptosense® assay (Peviva AB, Bromma, Sweden) specifically measures a neo-epitope formed by caspase-cleavage of CK18 at Asp396 (CK18Asp396-NE M30 neo-epitope) and reflects apoptotic cell death. This assay provides a specific method for discriminating between apoptotic and necrotic cell death [54]. The M65® ELISA (Peviva AB, Bromma, Sweden) measures soluble CK18 released from dying cells and can be used to assess overall death of epithelial cells due to both apoptosis and necrosis. The units of the two assays have been calibrated against identical standard material so that a ratio between caspase-cleaved and total CK18 can be calculated (M30:M65 ratio). Induction of apoptosis in cultured cells leads to release of caspase-cleaved CK18 and relatively high M30:M65 ratios, whereas induction of necrosis results almost exclusively in release of CK18 molecules that have not been cleaved by caspases and in a low M30:M65 ratio. The M30:M65 ratio, therefore, reflects the type of cell death.

It is important to mention that caspase-cleaved CK18 could also be detected *in vivo* by immunohistochemistry [42]. Recently, this technique has been widely used as a pharmacodynamic biomarker of cell death induced by a variety of different chemotherapeutic agents for different types of cancer [54]. The protocol for detecting total CK18 and CK18Asp396-NE can be found at www.peviva.se (Peviva AB, Bromma, Sweden).

6. Methods for analysis of cell–cell interactions

Recognition and clearance of dying cells is a complex and dynamic process coordinated by the interplay between ligands on dying cell, bridging molecules, and receptors on engulfing cells [2]. Dying cells can be cleared by professional phagocytes, such as macrophages and immature DCs, or by non-professional phagocytes, such as endothelial cells, fibroblasts, smooth cells, and epithelial cells. Efficient clearance of cells undergoing either apoptotic or necrotic cell death is crucial for normal homeostasis and for the modulation of immune responses [47]. In this section we will describe an *in vitro* phagocytosis assay for analysis of cell–cell interactions between macrophages and dying cells. We will also describe a two-parameter flow fluorocytometry phagocytosis assay to quantify uptake: scanning electron microscopy to study surface changes of phagocytes during engulfment, and transmission electron and fluorescence microscopy in combination with fluid phase markers to distinguish between the different internalization mechanisms used by macrophages to engulf apoptotic and necrotic cells.

6.1. In vitro phagocytosis assay by flow fluorocytometry

Technical limitations and differences in experimental approaches have hindered elucidation of the process of dying cell clearance. Many studies use fluorescence micros-

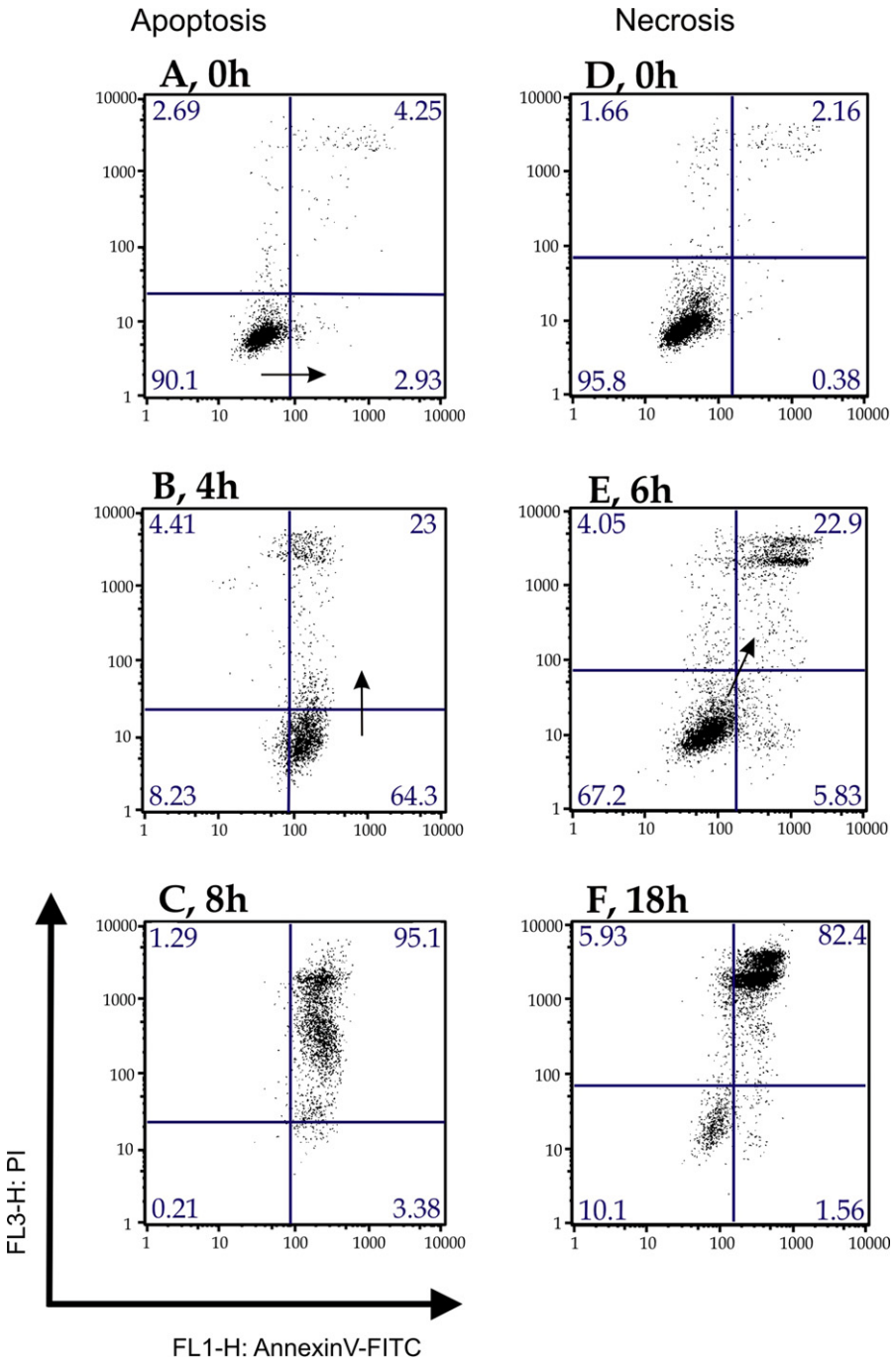

Fig. 3. Analysis of PS exposure versus cell permeability by flow fluorocytometry. During apoptosis there is a lag time between PS positivity and PI, but in necrosis these events coincide. Membrane changes leading to PS exposure occur rapidly in apoptosis, and the cell population shifts from the lower left quadrant (PI-negative/Annexin V-negative cells, A) to the lower right quadrant (PI-negative/Annexin V-positive cells, B). After PS exposure to the outer leaflet of the cell membrane, cells start loosing their membrane integrity, and the population shifts to the upper right quadrant (PI-positive/Annexin V-positive cells, C). During necrosis, PS exposure coincides with the permeabilization of the outer cell membrane. Consequently, cells immediately move from the lower left quadrant (PI-negative/Annexin V-negative cells, D) to the upper right quadrant of the dot blot (PI-positive/Annexin V-positive cells, E and F) without passing though the intermediate PI-negative/Annexin V-positive stage. L929sAhFas fibrosarcoma cells were pretreated for the indicated durations either with anti-Fas antibody or mTNF.

copy to quantify the uptake of dying cells, by counting the pre-stained ingested target cells inside the phagocytes in several microscopic fields. Obviously, this technique is labor intensive, time consuming and has a subjective component. To overcome these limitations and to explore the recognition and engulfment of dying cells by macrophages, we developed a quantitative, objective approach. The protocol described below uses a two-parameter flow fluorocytometry phagocytosis assay to quantify the percent of dying cell clearance. This procedure is based on staining

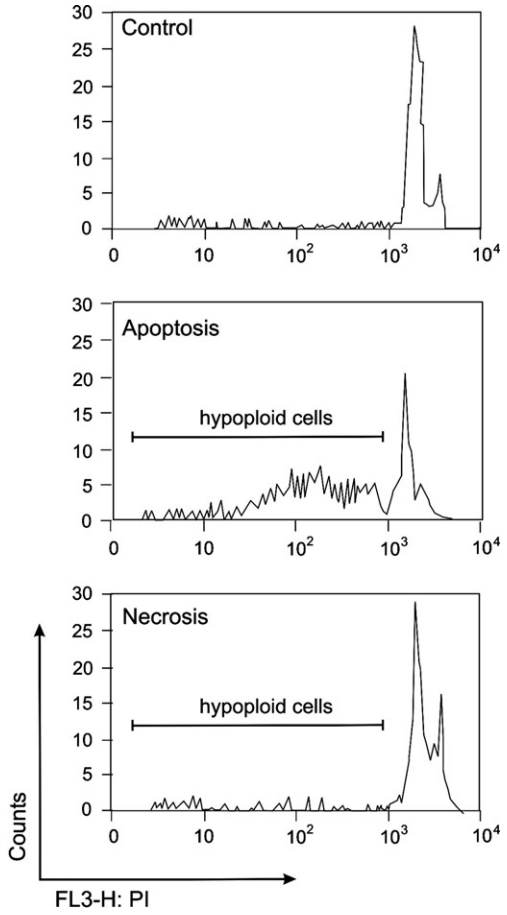

Fig. 4. A schematic representation of DNA fragmentation analysis by flow fluorocytometry. Live non-dividing cells exhibit a clear diploid DNA peak (2n, G1), whereas dividing cells give rise to a tetraploid peak (4n, G2). A non-synchronized, live population of cells has a typical biphasic peak of 2n (G1) and 4n (G2) cells (top). The DNA is fragmented and partially lost during apoptosis due to the formation of apoptotic bodies. Therefore, apoptotic cells (middle) are characterized by a hypoploid DNA fluorescence pattern (''sub-G1'' peak) compared to necrotic cells (bottom), which maintain their entire DNA content in the nucleus.

L929sAhFas target cells with Cell Tracker Green and Mf4/4 phagocytes with Cell Tracker Orange. These reagents pass through cell membranes, but inside the cell they are transformed into cell-impermeant reaction products. Mf4/4 phagocytes were characterized elsewhere [55].

6.1.1. Sample preparation

On day zero the cells are detached from the culture flasks with Enzyme Free Cell Dissociation Buffer (Gibco BRL), and 10–20 $\times$ 10^6 L929sAhFas and Mf4/4 cells are transferred to 15-ml tubes containing complete media and centrifuged for 5 min at 250*g*. After the supernatant is removed the cells are resuspended in 10 ml of serum-free medium and centrifuged again for 5 min at 250*g*. The cell pellet is resuspended in serum-free medium containing pre-diluted dyes. The target cells and phagocytes are stained with 0.8 μM Cell Tracker Green and 10 μM Cell Tracker Orange, respectively, for 30 min with rotation at 37 °C. Cell Tracker Green and Cell Tracker Orange (Molecular Probes, Invitrogen) are prepared as 10 mM stock solutions in sterile DMSO. Cell Tracker Green and Cell Tracker Orange have Abs 492 nm/Em 517 nm and Abs 541 nm/Em 565 nm, respectively. After staining, the cells are washed twice with complete medium and centrifuged for 5 min at 250*g*. They are next resuspended in 10 ml of complete medium and incubated for 30 min at 37 °C with rotation. At this step it is advisable to count the macrophages and target cells. The day before coculture, the cells are seeded: the target cells, e.g. L929sAhFas, at 2.5 $\times$ 10^5 cells per well in uncoated 24-well suspension tissue culture plate, and Mf4/4 cells at 2.5 $\times$ 10^5 cells per well in 24-well adherent plates. The target cells are grown in suspension plates so that the dying cells can be transferred easily to the wells containing attached phagocytes. The following day cell death is induced in target cells. Apoptosis and necrosis can be induced in L929sAhFas with anti-Fas antibodies (2 h, 125 ng/ml) and mTNF (5 h, 1000 IU/ml), respectively. To control cell death induction it is advisable to seed target cells in parallel for flow fluorocytometric analysis as described in Sections 2.2 and 3.1. After stimulation, target cells are collected, washed twice in the same medium in which macrophages are seeded, and counted to obtain the desired ratio of target cells to phagocytes. The ratio of target cells to macrophages should be the same in all samples. The target cells are added to the phagocytes and cocultured for at least 30 min. Time kinetics should be done when analyzing dead cell clearance. After coculture, target cells that have not been ingested are carefully washed away with PBS, and the phagocytes are detached with Enzyme Free Cell Dissociation Buffer (Gibco BRL). Following centrifugation for 5 min at 250*g* (4 °C) and re-suspension in ice-cold PBS, the samples are analyzed by flow fluorocytometry. During analysis the cells should be kept on ice and protected from light.

Apoptotic cells are taken up more rapidly and efficiently then necrotic cells [56]. Fig. 5 shows a dot plot representation of a flow fluorocytometric analysis of coculture of Mf4/4 cells with target cells. Target cells were treated as follows: untreated control; anti-Fas 125 ng/ml, 2 h (apoptotic cell death); and TNF 1000 IU/ml, 5 h (necrotic cell death). Single positive Mf4/4 cells (red) and free target cells (green) accumulate in regions I and III, respectively. After engulfing dying cells, macrophages become double positive (red and green) and accumulate in region II. The percentage of double-stained macrophages out of the whole macrophage population reflects the fraction of the macrophage population involved in clearance of target cells (percent phagocytosis) (Fig. 5). Moreover, the increase in mean green fluorescence could be used as an estimate of the amount cleared by phagocytes.

6.2. Analysis of internalization mechanisms

Two types of endocytosis have been observed so far. One is internalization of large particles by phagocytosis,

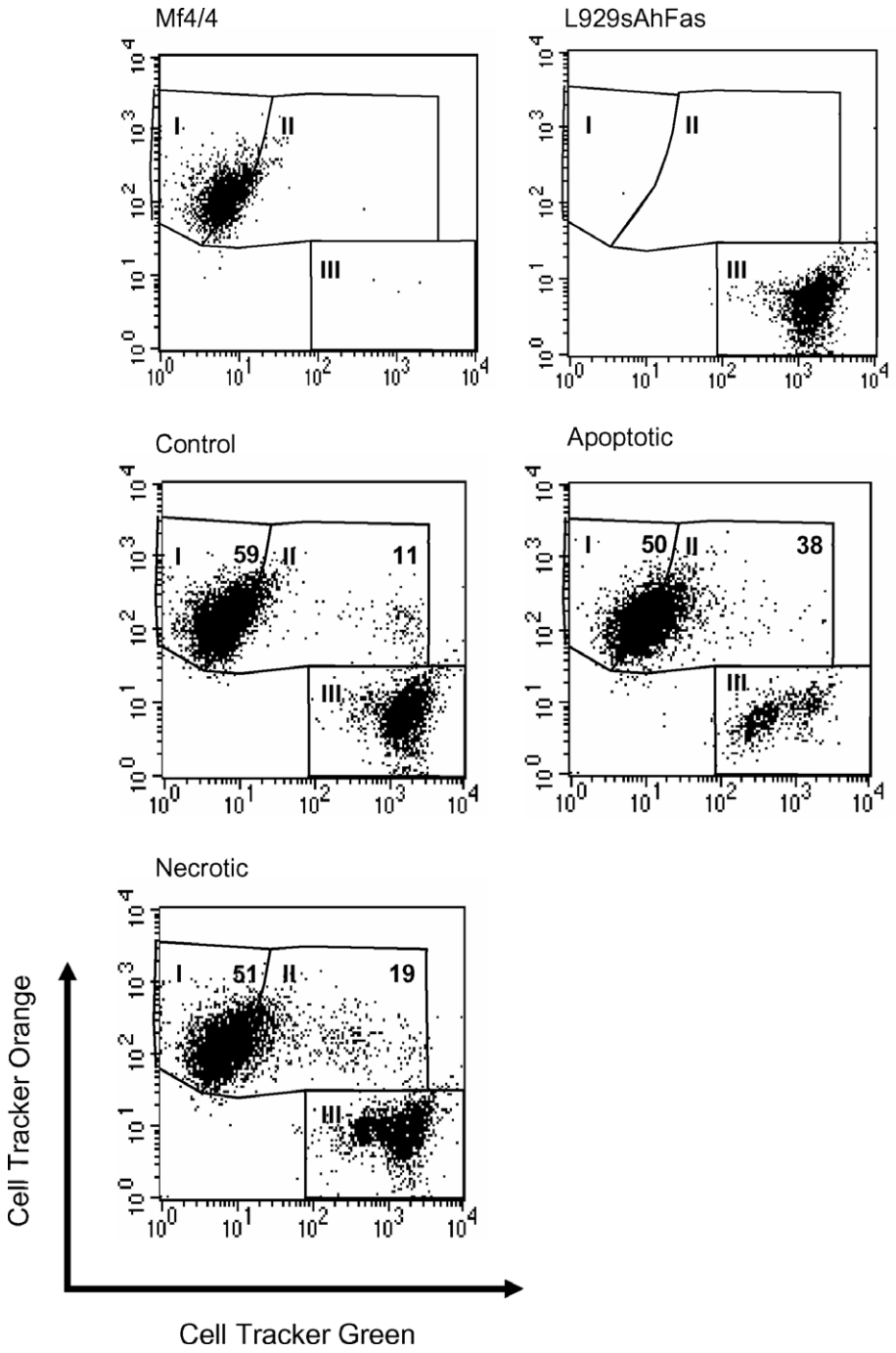

Fig. 5. Flow fluorocytometric analysis of uptake of apoptotic and necrotic cells by the Mf4/4 macrophage cell line. Dot plot representation of flow fluorocytometric analysis of Cell Tracker Orange-stained Mf4/4 cells after 2 h coincubation with Cell Tracker Green-stained target cells treated as follows: untreated (control); 2 h anti-Fas (apoptotic); and 5 h TNF (necrotic). Mf4/4 cells accumulate in regions I (no uptake) and II (uptake) and free target cells in region III. The calculated percentage of double-positive Mf4/4 cells (% uptake) for control (16%), apoptotic (43%) and necrotic (27%) cells indicates the extent to which macrophages are engaged in phagocytosis.

and the other is fluid phase uptake of small particles. Fluid phase uptake can occur by two distinct mechanisms, either micropinocytosis, which is the ingestion of small vesicles via clathrin-coated pits, or macropinocytosis via pinosomes (>0.2 μm diameter) formed by membrane ruffling [57–59]. Fluid-phase pinocytosis is usually studied by detecting the cellular accumulation of different soluble and impermeant probes, such as lucifer yellow (LY) and horseradish peroxidase (HRP) [60–64]. We recently developed a method involving coculture of phagocytes and target dying cells in the presence of fluid phase markers. This technique enables us to demonstrate that apoptotic cells are internalized by a zipper-like mechanism, whereas necrotic cells are taken up by macropinocytosis [65,66]. The use of fluid

phase markers (horseradish peroxidase and lucifer yellow) in combination with microscopic examination is important for accurately distinguishing between these internalization mechanisms: if the fluid phase markers are not colocalized with the ingested material within the same compartment, then a zipper-like mechanism of phagocytosis was used. Intracellular distribution of LY can be monitored in cocultures of macrophages and target cells by fluorescence microscopy, and HRP by light and transmission electron microscopy. Transmission electron microscopy is the method of choice for determining whether ingested material is localized in spacious macropinosomes or in tightly fitting phagosomes. Below we describe the use of fluid phase markers to discriminate between the distinct mechanisms macrophages use to engulf apoptotic and necrotic cells (Fig. 6). As a quantitative control, FACS assay should always be performed as described in Section 6.1. But first we will start by describing a protocol for scanning electron microscopy (SEM) because it can be used as a supplementary method for characterization of the surface changes of macrophages during internalization of dying cells.

6.2.1. Scanning electron microscopy

6.2.1.1. Sample preparation. Target cells are stimulated and a coculture of phagocytes with target cells at a given ratio is established as described in Section 6.1. In this protocol unstained cells can be used. However, a flow fluorocytometric assay should always be performed as described in Section 6.1 to obtain an idea of percent engulfment. After coincubating macrophages with target cells in a 1:1 ratio for 2 h, the cells are briefly washed with pre-warmed PBS and fixed in the 24-well plate for 1 h by immersion in pre-warmed (37 °C) SEM fixation buffer (2% glutaraldehyde containing 0.1 M sucrose buffered with 0.1 M Na-cacodylate, pH 7.2). Following fixation, the samples are rinsed twice in 0.15 M Na-cacodylate HCl buffer and post-fixed for 90 min in 1% OsO_4 in 0.15 M Na-cacodylate HCl buffer at room temperature. Then the specimens are dehydrated in a graded series of ethanol: 30% for 5 min, 50% for 5 min, 70% for 10 min, 85% for 10 min, 95% for 10 min, and 100% for 10 min, and then subjected to critical point drying from liquid CO_2. Finally, the samples are mounted on SEM stubs and examined by SEM.

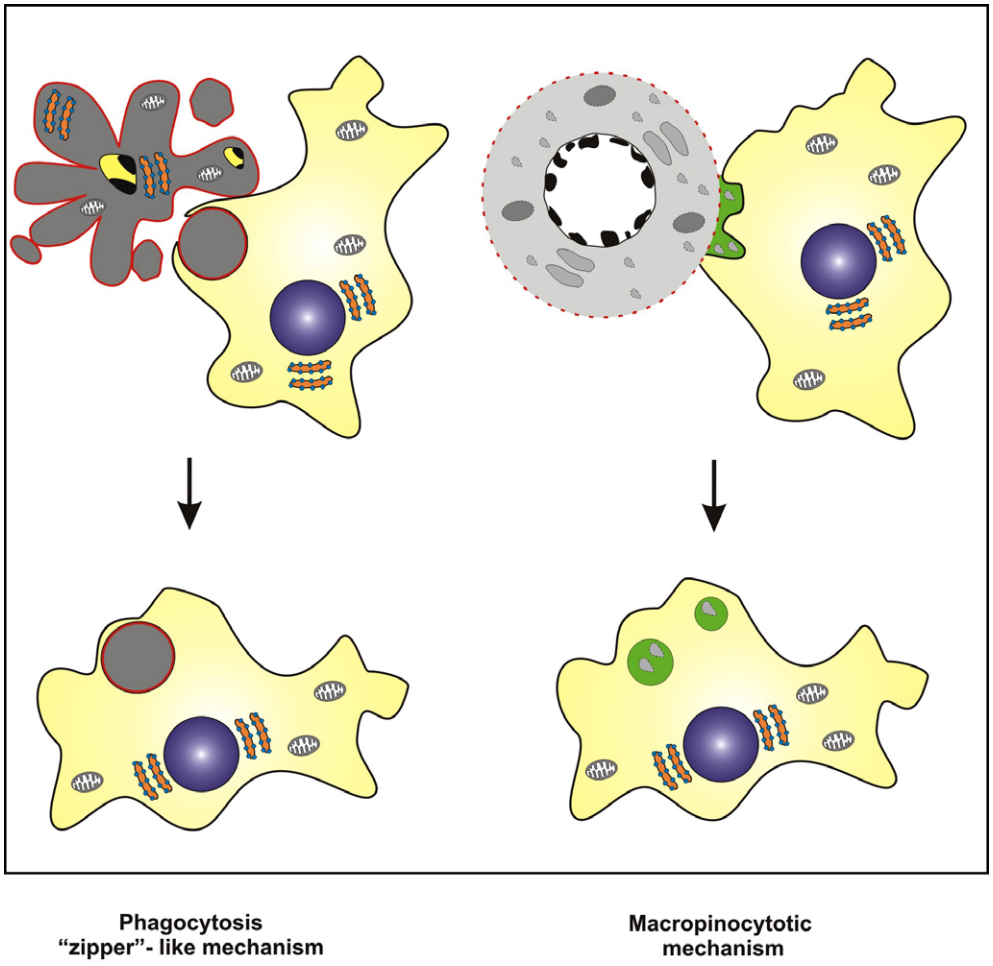

Fig. 6. A scheme of internalization mechanisms used by macrophages to engulf apoptotic and necrotic cells. Apoptotic cells are internalized by formation of tight fitting phagosomes that exclude lucifer yellow, a fluid phase marker. In contrast, necrotic cell material is internalized by macrophages with formation of spacious macropinosomes that also contain lucifer yellow (green staining). (For interpretation of the references to color in this figure legend, the reader is referred to the web version of this paper.)

SEM can reveal morphological characteristics typical of macropinocytosis or of the zipper-like mechanism of internalization. Macrophages using a zipper-like mechanism normally display narrow pseudopods extending over the surface of ingested particles (e.g. apoptotic bodies) and enclosing them on all sides. These morphological features are highly indicative of the formation of tight fitting phagosomes. Macrophages during macropinocytosis demonstrate irregular surface changes and formation of membrane ruffles, which are indicative of the formation of spacious macropinosomes and co-ingestion of extracellular fluid. In order to accurately discriminate between macropinocytosis and the zipper-like mechanism of internalization, and to have functional data, it is important to use fluid phase markers such as LY and HRP. These approaches are discussed next.

6.2.2. Transmission electron microscopy in combination with horseradish peroxidase

6.2.2.1. Sample preparation. Cells are seeded and cell death is induced in target cells as described in Section 6.1. Unstained cells could be used in this protocol. HRP is added simultaneously with the target cells to the adherent cultures of phagocytes to a final concentration 1 mg/ml, and incubated for 2 h at 37 °C. After coincubation, the cocultures of macrophages and target cells are rinsed with PBS buffer and fixed on ice for 1 h by immersion in TEM fixation buffer (2% glutaraldehyde containing 1 mM $CaCl_2$ and 0.1 M sucrose buffered with 0.1 M Na-cacodylate, pH 7.4). After the fixation and several washes in 0.1 M Na-cacodylate buffer (pH 7.4), the presence of HRP is revealed by incubating the samples at 37 °C in Tris-buffer (pH 7.6) containing 0.05 M DAB, 0.1% H_2O_2 and 1 mg of aminotriazole to block endogenous catalase activity. The localization of HRP is revealed cytochemically by the following oxidation reaction: $HRP + H_2O_2 + DAB \rightarrow HRP + 2H_2O +$ oxidized DAB (brownish staining). After that, the samples are washed in Tris-buffer containing 7.5% sucrose and osmicated overnight in 2% OsO_4 in the same buffer without sucrose. At this step brownish staining is converted to a black electron dense material due to the reaction between osmium tetroxide and oxidized DAB. Following dehydration in a graded series of ethanol (70%, 85%, 95%, 100%; 10 min each), the samples are infiltrated with a mixture of ethanol and LX-112 resin (Ladd Research Industries, USA) as follows: 1:1 for 30 min and 1:2 for 30 min. It is finally infiltrated with pure resin for 120 min and then polymerized for at least 48 h at 60 °C. The plastic is broken from the polymerized block and sawed into pieces to fit the ultramicrotome holders. Any remaining plastic bits are removed from the cutting surface. Semi-thin sections of 2 μm are cut and contrasted with toluidine blue (0.1%) to examine the quality of cocultures and to select an area for ultrathin sections. After that, ultrathin sections of 60 nm are cut and mounted on formvar-coated 100-mesh copper grids. The grids are evaporated in a JEOL (JEC-530) autocarboncoater at 4 V for 3 s and stained with uranyl acetate (7.5% in bi-distilled water, 1 drop per grid for 20 min) and Reynold's lead citrate (1 drop per grid for 10 min). Now the samples are ready for examination under the TEM.

6.2.3. Fluorescence microscopy in combination with lucifer yellow

Target cells are stimulated as described in Section 6.1. Lucifer yellow CH lithium salt (Molecular Probes, Invitrogen; final concentration 1 mg/ml) is added simultaneously with target cells labeled with Cell Tracker Orange (10 μM, prepared as described in Section 6.1) to the unlabeled adherent cultures of phagocytes and cocultured for 2 h at 37 °C. It is advisable to seed phagocytes on insertion glasses to make preparation for the microscope easier. After coincubation, adherent cocultures are rinsed five times with PBS and fixed in fixation buffer (3.8% freshly prepared paraformaldehyde in PBS, pH 7.4) for 15 min at room temperature. The adherent cocultures are rinsed three times in PBS and mounted on coverslips using Vectashield mounting medium for fluorescence with DAPI H-1200 (Vector Burlingame). DIC and fluorescence images are obtained with a confocal microscope. To detect staining, the following filter sets are used: for lucifer yellow BP 470/40, FT 500, 525/50; for Cell Tracker Red BP 515/560, FT 580, LP 590; for DAPI BP 340–380, FT 400, LP 425. It is advisable to take images at different *z*-levels for obtaining 3D information. Blind de-convolution (MLE-algorithm) and 3D rotations using the Leica Deblur software are performed. Since primary and secondary necrotic cells could show some background staining, quantify LY fluorescence of primary and secondary necrotic cells by determining the average fluorescence intensity, and then correct all images for background staining using the Metamorph 5.0 software or free software Image J (http://rsb.info.nih.gov/ij/).

7. Concluding remarks

Distinguishing necrosis from apoptosis should never be based on either morphological or biochemical criteria alone, but rather should take into account and integrate all available data. Accumulating evidence supports the concept that necrotic cell death is programmed. Therefore, unraveling molecular players and defining biochemical pathways in necrosis will provide us with powerful and specific methods for necrotic cell identification and help us to distinguish it positively from other forms of cell death. Many other interesting results are expected on the biochemical, cellular and (patho) physiological aspects of necrotic cell death.

Acknowledgments

We thank Wim Drijvers for the artwork and Dr. Amin Bredan for editing the manuscript. Dr. Dmitri V. Krysko is paid by a postdoctoral fellowship from the BOF (Bijzonder

Onderzoeksfonds 01P05807), Ghent University, and Dr. Tom Vanden Berghe is paid by a postdoctoral fellowship from FWO (Fonds Wetenschappelijk Onderzoek—Vlaanderen). This work has been supported by Flanders Institute for Biotechnology (VIB) and several Grants from the European Union (EC Marie Curie Training and Mobility Program, FP6, ApopTrain, MRTN-CT-035624; EC RTD Integrated Project, FP6, Epistem, LSHB-CT-2005-019067), the Interuniversity Poles of Attraction-Belgian Science Policy (IAP6/18), the Fonds voor Wetenschappelijk Onderzoek—Vlaanderen (3G.0218.06), and the Special Research Fund of Ghent University (Geconcerteerde Onderzoekstacties 12.0505.02).

Appendix A. Supplementary data

Supplementary data associated with this article can be found, in the online version, at doi:10.1016/j.ymeth.2007.12.001.

References

[1] G. Kroemer, W.S. El-Deiry, P. Golstein, M.E. Peter, D. Vaux, P. Vandenabeele, B. Zhivotovsky, M.V. Blagosklonny, W. Malorni, R.A. Knight, M. Piacentini, S. Nagata, G. Melino, Cell Death Differ. 12 (Suppl. 2) (2005) 1463–1467.
[2] D.V. Krysko, K. D'Herde, P. Vandenabeele, Apoptosis 11 (2006) 1709–1726.
[3] L.E. Munoz, U.S. Gaipl, S. Franz, A. Sheriff, R.E. Voll, J.R. Kalden, M. Herrmann, Rheumatology (Oxford) 44 (2005) 1101–1107.
[4] R.W. Vandivier, V.A. Fadok, P.R. Hoffmann, D.L. Bratton, C. Penvari, K.K. Brown, J.D. Brain, F.J. Accurso, P.M. Henson, J. Clin. Invest. 109 (2002) 661–670.
[5] S. Hodge, G. Hodge, R. Scicchitano, P.N. Reynolds, M. Holmes, Immunol. Cell Biol. 81 (2003) 289–296.
[6] J.F. Kerr, A.H. Wyllie, A.R. Currie, Br. J. Cancer 26 (1972) 239–257.
[7] V.A. Fadok, D.R. Voelker, P.A. Campbell, J.J. Cohen, D.L. Bratton, P.M. Henson, J. Immunol. 148 (1992) 2207–2216.
[8] G. Denecker, D. Vercammen, M. Steemans, T. Vanden Berghe, G. Brouckaert, G. Van Loo, B. Zhivotovsky, W. Fiers, J. Grooten, W. Declercq, P. Vandenabeele, Cell Death Differ. 8 (2001) 829–840.
[9] G. Kroemer, J.C. Reed, Nat. Med. 6 (2000) 513–519.
[10] G. Van Loo, H. Demol, M. van Gurp, B. Hoorelbeke, P. Schotte, R. Beyaert, B. Zhivotovsky, K. Gevaert, W. Declercq, J. Vandekerckhove, P. Vandenabeele, Cell Death Differ. 9 (2002) 301–308.
[11] M. Enari, H. Sakahira, H. Yokoyama, K. Okawa, A. Iwamatsu, S. Nagata, Nature 391 (1998) 43–50.
[12] M.C. Maiuri, E. Zalckvar, A. Kimchi, G. Kroemer, Nat. Rev. Mol. Cell Biol. 8 (2007) 741–752.
[13] I. Tanida, T. Yamaji, T. Ueno, S. Ishiura, E. Kominami, K. Hanada, Autophagy 4 (2007).
[14] I. Tanida, T. Ueno, E. Kominami, Int. J. Biochem. Cell Biol. 36 (2004) 2503–2518.
[15] N. Mizushima, T. Yoshimori, Autophagy 3 (2007) 542–545.
[16] G. Majno, I. Joris, Am. J. Pathol. 146 (1995) 3–15.
[17] T. Vanden Berghe, W. Declercq, P. Vandenabeele, Mol. Cell 26 (2007) 769–771.
[18] N. Festjens, T. Vanden Berghe, P. Vandenabeele, Biochim. Biophys. Acta 1757 (2006) 1371–1387.
[19] W.X. Zong, C.B. Thompson, Genes Dev. 20 (2006) 1–15.
[20] J. Yuan, Mol. Cell 23 (2006) 1–12.
[21] D. Vercammen, P. Vandenabeele, R. Beyaert, W. Declercq, W. Fiers, Cytokine 9 (1997) 801–808.
[22] P.N. Unwin, G. Zampighi, Nature 283 (1980) 545–549.
[23] P.N. Unwin, P.D. Ennis, Nature 307 (1984) 609–613.
[24] M.C. Cummings, C.M. Winterford, N.I. Walker, Am. J. Surg. Pathol. 21 (1997) 88–101.
[25] E. Falcieri, P. Gobbi, A. Cataldi, L. Zamai, I. Faenza, M. Vitale, Histochem. J. 26 (1994) 754–763.
[26] J.F. Kerr, C.M. Winterford, B.V. Harmon, Cancer 73 (1994) 2013–2026.
[27] A.H. Wyllie, in: I.D.B.R.A. Lockshin (Ed.), Cell Death in Biology and Pathology, Springer, Berlin, 1981, pp. 9–34.
[28] P. Williamson, R.A. Schlegel, Biochim. Biophys. Acta 1585 (2002) 53–63.
[29] S. Zullig, L.J. Neukomm, M. Jovanovic, S.J. Charette, N.N. Lyssenko, M.S. Halleck, C.P. Reutelingsperger, R.A. Schlegel, M.O. Hengartner, Curr. Biol. 17 (2007) 994–999.
[30] G. Denecker, H. Dooms, G. Van Loo, D. Vercammen, J. Grooten, W. Fiers, W. Declercq, P. Vandenabeele, FEBS Lett. 465 (2000) 47–52.
[31] O. Krysko, L. De Ridder, M. Cornelissen, Apoptosis 9 (2004) 495–500.
[32] C. Van de Wiele, H. Vermeersch, D. Loose, A. Signore, N. Mertens, R. Dierckx, Cancer Biother. Radiopharm. 19 (2004) 189–194.
[33] C.M. Lahorte, J.L. Vanderheyden, N. Steinmetz, C. Van de Wiele, R.A. Dierckx, G. Slegers, Eur. J. Nucl. Med. Mol. Imaging 31 (2004) 887–919.
[34] U. Trahtemberg, M. Atallah, A. Krispin, I. Verbovetski, D. Mevorach, Apoptosis 12 (2007) 1769–1780.
[35] M. Lamkanfi, W. Declercq, B. Depuydt, M. Kalai, X. Saelens, P. Vandenabeele, in: H. Walczak (Ed.), Caspases: Their Role in Cell Death and Cell Survival, Landes Bioscience, Kluwer Academic Press, Georgetown, TX, 2003.
[36] D. Metivier, B. Dallaporta, N. Zamzami, N. Larochette, S.A. Susin, I. Marzo, G. Kroemer, Immunol. Lett. 61 (1998) 157–163.
[37] G. Kroemer, B. Dallaporta, M. Resche-Rigon, Annu. Rev. Physiol. 60 (1998) 619–642.
[38] J.J. Lemasters, A.L. Nieminen, T. Qian, L.C. Trost, S.P. Elmore, Y. Nishimura, R.A. Crowe, W.E. Cascio, C.A. Bradham, D.A. Brenner, B. Herman, Biochim. Biophys. Acta 1366 (1998) 177–196.
[39] S. Nagata, Cornea 21 (2002) S2–S6.
[40] S. Nagata, Exp. Cell Res. 256 (2000) 12–18.
[41] P.R. Walker, J. Leblanc, B. Smith, S. Pandey, M. Sikorska, Methods 17 (1999) 329–338.
[42] W.R. Duan, D.S. Garner, S.D. Williams, C.L. Funckes-Shippy, I.S. Spath, E.A. Blomme, J. Pathol. 199 (2003) 221–228.
[43] N.A. Thornberry, T.A. Rano, E.P. Peterson, D.M. Rasper, T. Timkey, M. Garcia-Calvo, V.M. Houtzager, P.A. Nordstrom, S. Roy, J.P. Vaillancourt, K.T. Chapman, D.W. Nicholson, J. Biol. Chem. 272 (1997) 17907–17911.
[44] R.V. Talanian, C. Quinlan, S. Trautz, M.C. Hackett, J.A. Mankovich, D. Banach, T. Ghayur, K.D. Brady, W.W. Wong, J. Biol. Chem. 272 (1997) 9677–9682.
[45] T. Vanden Berghe, M. Kalai, G. van Loo, W. Declercq, P. Vandenabeele, J. Biol. Chem. 278 (2003) 5622–5629.
[46] V. Stoka, B. Turk, S.L. Schendel, T.H. Kim, T. Cirman, S.J. Snipas, L.M. Ellerby, D. Bredesen, H. Freeze, M. Abrahamson, D. Bromme, S. Krajewski, J.C. Reed, X.M. Yin, V. Turk, G.S. Salvesen, J. Biol. Chem. 276 (2001) 3149–3157.
[47] D.V. Krysko, P. Vandenabeele, Cell Death Differ. 15 (2007) 29–38.
[48] T. Rae, J. Biomed. Mater. Res. 11 (1977) 839–846.
[49] P. Scaffidi, T. Misteli, M.E. Bianchi, Nature 418 (2002) 191–195.
[50] J.S. Park, D. Svetkauskaite, Q. He, J.Y. Kim, D. Strassheim, A. Ishizaka, E. Abraham, J. Biol. Chem. 279 (2004) 7370–7377.
[51] D. Yang, Q. Chen, H. Yang, K.J. Tracey, M. Bustin, J.J. Oppenheim, J. Leukoc. Biol. 81 (2007) 59–66.
[52] L. Apetoh, F. Ghiringhelli, A. Tesniere, M. Obeid, C. Ortiz, A. Criollo, G. Mignot, M.C. Maiuri, E. Ullrich, P. Saulnier, H. Yang, S. Amigorena, B. Ryffel, F.J. Barrat, P. Saftig, F. Levi, R. Lidereau, C. Nogues, J.P. Mira, A. Chompret, V. Joulin, F. Clavel-Chapelon, J. Bourhis, F. Andre, S. Delaloge, T. Tursz, G. Kroemer, L. Zitvogel, Nat. Med. 13 (2007) 1050–1059.

[53] E. Fuchs, K. Weber, Annu. Rev. Biochem. 63 (1994) 345–382.
[54] J. Cummings, T.H. Ward, A. Greystoke, M. Ranson, C. Dive, Br. J. Pharmacol. (2007).
[55] M. Desmedt, P. Rottiers, H. Dooms, W. Fiers, J. Grooten, J. Immunol. 160 (1998) 5300–5308.
[56] G. Brouckaert, M. Kalai, D.V. Krysko, X. Saelens, D. Vercammen, M. Ndlovu, G. Haegeman, K. D'Herde, P. Vandenabeele, Mol. Biol. Cell 15 (2004) 1089–1100.
[57] J.A. Swanson, S.C. Baer, Trends Cell Biol. 5 (1995) 89–93.
[58] J.A. Swanson, C. Watts, Trends Cell Biol. 5 (1995) 424–428.
[59] I. Torii, S. Morikawa, M. Nagasaki, A. Nokano, K. Morikawa, Immunology 103 (2001) 70–80.
[60] R.M. Steinman, Z.A. Cohn, J. Cell Biol. 55 (1972) 186–204.
[61] R.M. Steinman, J.M. Silver, Z.A. Cohn, J. Cell Biol. 63 (1974) 949–969.
[62] C.C. Norbury, L.J. Hewlett, A.R. Prescott, N. Shastri, C. Watts, Immunity 3 (1995) 783–791.
[63] C.C. Norbury, B.J. Chambers, A.R. Prescott, H.G. Ljunggren, C. Watts, Eur. J. Immunol. 27 (1997) 280–288.
[64] J.A. Swanson, J. Cell Sci. 94 (Pt 1) (1989) 135–142.
[65] D.V. Krysko, G. Brouckaert, M. Kalai, P. Vandenabeele, K. D'Herde, J. Morphol. 258 (2003) 336–345.
[66] D.V. Krysko, G. Denecker, N. Festjens, S. Gabriels, E. Parthoens, K. D'Herde, P. Vandenabeele, Cell Death Differ. 13 (2006) 2011–2022.